

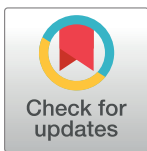
RESEARCH ARTICLE

Effects of glycosaminoglycan content in extracellular matrix of donor cartilage on the functional properties of osteochondral allografts evaluated by micro-CT non-destructive analysis

Yong Jun Jin^{1,2}, Do Young Park^{1,2}, Sujin Noh³, HyeonJae Kwon^{2,4}, Dong Il Shin^{2,4}, Jin Ho Park^{2,4}, Byoung-Hyun Min^{1,2,4*}

1 Department of Orthopedic Surgery, School of Medicine, Ajou University, Suwon, Republic of Korea, **2** Cell Therapy Center, Ajou University Medical Center, Suwon, Republic of Korea, **3** Department of Biomedical Sciences, Graduate School of Ajou University, Suwon, Republic of Korea, **4** Department of Molecular Science and Technology, Ajou University, Suwon, Republic of Korea

* bhmin@ajou.ac.kr



OPEN ACCESS

Citation: Jin YJ, Park DY, Noh S, Kwon H, Shin DI, Park JH, et al. (2023) Effects of glycosaminoglycan content in extracellular matrix of donor cartilage on the functional properties of osteochondral allografts evaluated by micro-CT non-destructive analysis. PLoS ONE 18(5): e0285733. <https://doi.org/10.1371/journal.pone.0285733>

Editor: Carlos Alberto Antunes Viegas, Universidade de Trás-os-Montes e Alto Douro: Universidade de Trás-os-Montes e Alto Douro, PORTUGAL

Received: January 6, 2023

Accepted: April 28, 2023

Published: May 23, 2023

Peer Review History: PLOS recognizes the benefits of transparency in the peer review process; therefore, we enable the publication of all of the content of peer review and author responses alongside final, published articles. The editorial history of this article is available here: <https://doi.org/10.1371/journal.pone.0285733>

Copyright: © 2023 Jin et al. This is an open access article distributed under the terms of the [Creative Commons Attribution License](https://creativecommons.org/licenses/by/4.0/), which permits unrestricted use, distribution, and reproduction in any medium, provided the original author and source are credited.

Abstract

Osteochondral allograft (OCA) is an important surgical procedure used to repair extensive articular cartilage damage. It is known that chondrocyte viability is crucial for maintaining the biochemical and biomechanical properties of OCA, which is directly related to the clinical success of the operation and is the only standard for preoperative evaluation of OCA. However, there is a lack of systematic research on the effect of the content of cellular matrix in OCA cartilage tissue on the efficacy of transplantation. Therefore, we evaluated the effect of different GAG contents on the success of OCA transplantation in a rabbit animal model. Each rabbit OCA was treated with chondroitinase to regulate glycosaminoglycan (GAG) content in the tissue. Due to the different action times of chondroitinase, they were divided into 4 experimental groups (including control group, 2h, 4h, and 8h groups). The treated OCAs of each group were used for transplantation. In this study, transplant surgery effects were assessed using micro-computed tomography (μ CT) and histological analysis. Our results showed that tissue integration at the graft site was poorer in the 4h and 8h groups compared to the control group at 4 and 12 weeks in vivo, as were the compressive modulus, GAG content, and cell density reduced. In conclusion, we evaluated the biochemical composition of OCAs before and after surgery using μ CT analysis and demonstrated that the GAG content of the graft decreased, it also decreased during implantation; this resulted in decreased chondrocyte viability after transplantation and ultimately affected the functional success of OCAs.

1. Introduction

Articular cartilage defect is a common orthopedic disease [1, 2]. Cartilage is limited in its ability to repair itself due to insufficient vascular supply and the inability of differentiated cell

Data Availability Statement: All relevant data are within the paper and its [Supporting information files](#).

Funding: This study was supported by the Korea Health Technology R&D Project (HI17C2191) through the Korea Health Industry Development Institute, funded by the Ministry of Health & Welfare. We have no potential conflict of interest relevant to this article. The funders had no role in study design, data collection and analysis, decision to publish, or preparation of the manuscript. This study was approved by the IACUC (IACUC No.2021-0030) at the Laboratory of Animal Research at Aju University Medical Center.

Competing interests: The authors have declared that no competing interests exist.

populations to respond to injury [3, 4]. Therefore, the treatment of articular cartilage defects remains a challenging clinical problem. Surgical options currently used clinically for articular cartilage repair include microfracture, autologous chondrocyte implantation, osteochondral autograft, and allograft transplantation [5]. Especially for large areas of full-thickness articular cartilage lesions (>3cm²), osteochondral allograft (OCA) transplantation has unique advantages [6–8]. OCA contains available chondrocytes and hyaline cartilage-related matrix for direct transplantation into the defect site [9]. In the most recent data for fresh OCA transplantation on the femoral condyle, the 5-year survival rate of chondrocytes was between 90% and 95%, the 10-year survival rate was around 85%, and the 15-year survival rate was more than 70% [10, 11]. Furthermore, the survival rate of chondrocytes is an important factor in the long-term functional maintenance of OCA [12, 13].

Although many studies have demonstrated clinical efficacy of OCA transplantation in osteochondral defects, procedures such as pre-transplant donor matching and the diagnosis of pathogen that could transmit required at least 2 weeks, which limits the transplantation efficiency [14, 15]. Studies have revealed that chondrocyte viability is critical for maintaining the biochemical and biomechanical characteristics of OCA, which the only criterion for preoperative assessment of OCA and directly related to the clinical success of the surgery [13, 16–19]. Therefore, a number of graft storage methods including cryopreservation have been suggested to ensure the functional integrity of chondrocytes and ECM in OCA [16, 20–23].

Articular cartilage ECM regulates chondrocyte function through cell-matrix interactions, building cytoskeleton and integrin-mediated signal transduction [24]. Given its chondroinductive properties, many decellularized cartilage matrices are used for cartilage regeneration, such as Zimmer's Chondrofix[®] osteochondral allograft products [25]. Therefore, the ECM content of donor cartilage is also an important factor affecting the success of implantation in OCA transplantation. Under normal physiological conditions of articular cartilage, homeostasis and turnover of the ECM is dependent on the responses of chondrocytes to self and paracrine anabolic and catabolic pathways [26, 27]. For example, chondrocytes regulate the synthesis of proteoglycans and type II collagen by controlling growth factors and cytokines [28, 29]. Likewise, the ECM is a complex network that surrounds chondrocytes and is highly fluid. It is composed of protein and proteoglycan components and generates biochemical and biomechanical signals to chondrocytes, thereby regulating cellular processes including growth, differentiation, migration, homeostasis, survival and morphogenesis [30]. An integrated ECM structure maintains the stability of the extracellular microenvironment, thereby preventing cellular damage and apoptosis [31]. Therefore, the integrity of the ECM of the cartilage tissue in the graft is also an important factor for successful OCA function after transplantation.

GAG is an important component of articular cartilage ECM, and it is an important detection marker in various physiological and pathological stages of articular cartilage [32, 33]. Among the biomechanical functions of the ECM, GAGs form a stress-strain fluid flow microenvironment by regulating osmotic pressure and chemical expansion stress effects in the tissue, and play a buffering mechanism in cartilage tissue, ultimately preventing cell damage [34–36]. Moreover, the negatively charged GAG binds to interstitial water to provide bio-compression stiffness [37, 38]. This function maintains the stability of the extracellular microenvironment when the cartilage tissue is subjected to continuous pressure load [39, 40]. Interestingly, this negatively charged characteristic of GAG provides us with a non-destructive analysis method using μ CT to calculate the GAG content in the graft, thus confirming the results of several previous studies [38, 41–43]. This leads to novel directions for a new detection mode for the process of graft quality control.

In general, achieving successful results after OCA implantation is closely related to donor cartilage cells, but the role played by GAG content in the donor cartilage tissue has yet to be

fully elucidated. We hypothesized that maintaining a high GAG content in the graft might be an important factor for the functional success of OCA after implantation. Therefore, the purpose of this study was to determine the importance of the GAG content of the donor cartilage tissue for implantation success in rabbit model by using the μ CT non-destructive analysis method.

2. Materials and methods

2.1 Experimental design

Fig 1 shows an overview of the experimental strategy. OCAs with a diameter of 3.5 mm were obtained from femoral trochlear parts of bilateral knee in New Zealand white rabbits (weight 2.5–3.0 kg), and the grafts were then treated with chondroitinase ABC (Sigma-Aldrich, USA). The experiments were divided into four groups according to the time of chondroitinase treatment; Group 1: control (grafts were not treated with chondroitinase; untreated group), Group 2: 2h group (grafts received 2 hours of chondroitinase treatment), Group 3: 4h group (grafts received 4 hours chondroitinase treatment), and Group 4: 8h group (grafts received 8 hours chondroitinase treatment). This experiment is divided into two separate parts. In the previous part, the correlation between μ CT values and GAG content were determined by analyzing μ CT value, GAG content, cell viability and histological staining of OCA at in vitro study. As a preliminary in vivo study (with the following part of the same surgical approach), the OCA of the graft site was obtained and analyzed for μ CT and GAG content and at 4 and 12 weeks postoperatively. In the latter part, μ CT analysis was performed on OCA obtained from donors and then implanted into subjects to demonstrate the influence of GAG content on the functional success of the graft. Biomechanics, radiology, histology, and cell viability were examined at 4 and 12 weeks postoperatively to determine the effect of OCA transplantation.

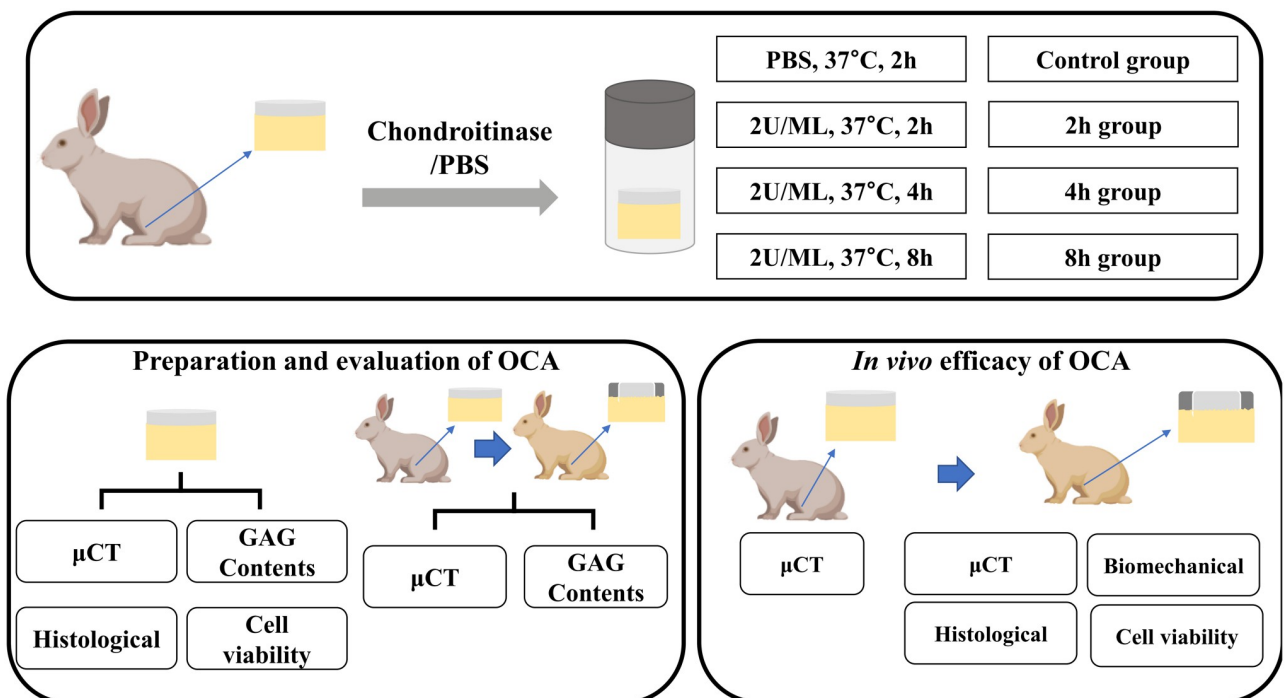


Fig 1. Simplified diagram of the overall research design.

<https://doi.org/10.1371/journal.pone.0285733.g001>

2.2 Preparation and characterization of OCA

All experimental protocols involving animals were conducted under IACUC approval (IACUC No. 2021–0030) at the Laboratory of Animal Research at XXX University Medical Center. A total of 68 male New Zealand white rabbits (KOATECH, Pyeongtaek, Korea) were used; 44 were used for *in vitro* research, while the remaining 24 were used for preliminary *in vivo* tests. The rabbits were 12 weeks old and weighed 2.5–3.0 kg. OCAs with a diameter of 4 mm were obtained from the femoral trochlear parts of the bilateral knee joints of adult New Zealand male rabbits. After isolation, they were stored in phosphate-buffered saline (PBS) solution at room temperature. Each graft was then soaked to a medium containing 1 unit/ml chondroitinase at 37°C for 2, 4, or 8 hours according to the assigned group (while the control group received an 8-hour treatment of PBS solution). After the treatment, each OCA was washed for 5 minutes each in PBS solution three times. For preliminary *in vivo* experiments, OCAs were obtained from 12 donor rabbits and treated with chondroitinase as described above, then each group of OCAs were implanted into 12 subject rabbits. To analyze the OCA samples in terms of μ CT and GAG content, the graft sites were obtained 4 and 12 weeks after surgery.

2.2.1 Radiographic analysis of OCA. Iobrix Injection contrast agent (TAEJOON, South Korea) was applied to the OCA for 3 hours at room temperature. Then, the μ CT value of OCA was determined with a microcomputer tomography device (CT, Skyscan 1076, Skyscan, Belgium). The CT parameters were set to a resolution of 18.22 μ m pixels with an exposure time of 300 ms using a 40 kV energy source and a 200 mA current. The imaging and data analysis were conducted using Skyscan software (Skyscan, Belgium). This study used Hounsfield units (HU), which range from 0 to 3000 [38], to measure the average CT attenuation. To remove the components of the contrast agent in the tissue, each OCA was washed three times in PBS solution for five minutes each time following the μ CT analysis. Subsequently, we analyzed OCA for GAG content, cell viability, and histological staining.

2.2.2 Measurement of GAG contents in OCA. The cartilage tissue that separated from each OCA ($n = 4$) was freeze-dried and incubated with a papain digestion solution (5 mM L-cysteine, 100 mM Na₂HPO₄, 5 mM EDTA, and 125 mg/ml papain type III: Sigma-Aldrich, Missouri, USA) overnight at 60°C. At this point, a 1,9-dimethyl-methylene blue (DMMB) Blyscan™ Glycosaminoglycan test kit was used to determine the total sGAG content (b1000, bicolor, UK) followed by manufacturer's instruction.

2.2.3 Comparison of μ CT value and GAG quantification. In the present study, we reproduced the measurement of the GAG content of OCA by μ CT analysis. In order to confirm the correlation between the μ CT value and the GAG content after implantation of OCA *in vivo*, the following experiments were performed. Assuming that the mean CT value reflects the GAG content of the tissue, μ CT analysis and GAG content detection were performed on each group of grafts ($n = 64$, including 40 samples from *in vitro* experiments and 24 samples from 4 and 12 weeks of preliminary *in vivo* experiments). The experimental method described above was used to measure the μ CT value and GAG content of each graft; the relationship between the two values was analyzed, and R^2 (determination coefficient) was calculated to determine the applicable range and degree of effectiveness.

2.2.4 Cell viability measurement of OCA graft. After μ CT imaging, LIVE/DEAD cell staining (L3224, Thermo Fisher, USA) was conducted to determine the viability of the chondrocytes in each set of grafts ($n = 4$). A scalpel (1 mm) was used to cut a full-thickness cross-sectional slice of the cartilage. The cartilage slice was treated with the LIVE/DEAD working solution (2 μ M calcein-AM and 4 μ M ethidium homodimer-1 in PBS), which was then incubated for 1 hour at room temperature. Each cartilage slice was washed three times in PBS

before imaging by confocal microscopy (Zeiss LSM510 Meta). The percentage of chondrocyte viability for each graft was quantified using digital image analysis. As the mean viable chondrocyte density (cells/mm²) assessed from this graft is reported as the number of viable chondrocytes per graft [13], the area of the cartilage tissue was measured and the ratio of the number of live chondrocytes to the area of the cartilage was used to calculate the viable chondrocyte density.

2.2.5 Histologic analysis of OCA. After μ CT imaging, specimens were preserved for 7 days at room temperature in Neutral Buffered Formalin (NBF) at a concentration of 10%. Before being embedded in paraffin wax, the samples were decalcified with 5% nitric acid for 3 days ($n = 4$). 4 μ m thick slides of OCA were prepared and stained with Safranin O/Fast green. To determine the extent of cartilage repair, sections from five samples per group were scored blindly by three independent observers using the Histological Scoring System for Assessment of Cartilage Repair [44].

2.2.6 Biomechanical analysis. To evaluate the biomechanical characteristics of OCA in each group, samples were collected ($n = 4$), and compressive tests were performed in a versatile biomechanical system machine (testXpert III testing software, Zwick Roell, ProLine, Germany) equipped with a 1000N load cell. A fully automated series of compressive-relaxation steps (step 5 μ m, velocity 1 μ m/min) was repeated up to 50% strain. After a phase test, 60 seconds of relaxation was set as the criterion for the beginning of a new step. For each sample, the test was repeated three times, and the stress-strain curve were made. Finally, the compressive modulus was obtained from the slope of the 5–15% linear part of the stress-strain curve [45].

2.3 Preoperative evaluation

OCAs with dimensions of 3.5 mm diameter x 2.5 mm height were obtained from the donor's rabbit knee femoral trochlear parts using a special biopuncher. After conducting an evaluation by μ CT analysis and after three washes with PBS solution, OCAs were treated with chondroitinase and evaluated by μ CT analysis; finally, after 3 washes with PBS solution, the OCA implantation procedure was prepared. The above steps were all carried out under sterile conditions.

2.3.1 Animal model and surgical procedure. A total of 100 male New Zealand white rabbits (KOATECH, Pyeongtaek, Korea) aged 12 weeks (body weight 2.5–3.0 kg) were used. 50 rabbits were donors and the remaining 50 were operated on bilateral knee joints. 50 rabbits were divided into four experimental groups: Control group, 2h group, 4h group, and 8h group. The biomechanical tests ($n = 5$), histological analysis ($n = 5$) was performed in each group at 4 and 12 weeks after surgery, and cell survival analysis was performed 12 weeks after surgery ($n = 5$). The surgical procedure can be briefly described as follows: Each rabbit was anesthetized using Zoletil (10 mg/kg of zolazepam and tiletamine, Virbac Laboratoire) and Rompun (10 mg/kg of xylazine hydrochloride, Bayer Korea) (1:2 ratio, 1 mL/kg). After a skin incision under sterile conditions, a medial parapatellar approach was taken. A cylindrical defect with a diameter of 3.5 mm and a depth of 2.5 mm was produced in the exposed femoral trochlear, and the allograft system calibration press-fit method was used to randomly implant each group of prepared OCAs [46]. Each rabbit received an intramuscular injection of antibiotic (cefotaxime 1g in a dose of 150mg/kg/day) and analgesic (ketorolac 60 mg/day) for three days postoperatively. At 4 and 12 weeks after surgery, the rabbits were sacrificed, and knee samples were collected for further evaluation.

2.3.2 Gross morphological analysis. Gross morphological evaluation of each sample was performed immediately after animal sacrifice to evaluate defect filling, surface smoothness, and tissue integration. Samples were blindly scored by three independent evaluators based on the International Cartilage Research Society (ICRS) scoring system.

2.3.3 μ CT and μ CT GAG quantification analyses. At 4 and 12 weeks after surgery, all samples were collected and processed with Iobrix Injection contrast agent (TAEJOON, Korea), then used for μ CT imaging and analysis of data by Skyscan software (Skyscan, Belgium) to measure HU at the transplant site value. Further, the relative GAG content of each group was calculated by the linear regression diagram of μ CT value and GAG content. The contrast agent was then washed with PBS solution to prepare for the subsequent analysis experiments.

2.4 Statistical analysis

In this study, all quantitative datasets were expressed as mean \pm standard deviation (SD). Shapiro-Wilk test was used to confirm normality of all samples. Analysis of variance (ANOVA) was performed on standardized samples to compare parametric data between groups. Kruskal-Wallis test with Dunn's test was used to compare multiple groups when the data are not normally distributed. Two-way ANOVA and Bonferroni test were applied in the presence of two independent variables. All data analyses were performed using GraphPad Prism 8 (GraphPad Software, La Jolla, CA, USA) to determine whether the results for the various datasets were statistically significantly different, with a value of $P < 0.05$ considered to represent a significant difference (* $p < 0.05$, ** $p < 0.01$, *** $p < 0.001$).

3. Results

3.1 GAG contents and cell viability on OCAs

Fig 2 showed changes of GAG contents and cell viability after treating chondroitinase at time-dependent manner. After treating chondroitinase for 4 and 8 hours at 37°C, the GAG content was significantly reduced. (Control group—116.01 \pm 6.3 μ g/mg; 2h group—86.85 \pm 7.8 μ g/mg; 4h group—75.15 \pm 8.3 μ g/mg; and 8h group—59.34 \pm 5.1 μ g/mg.) The percentages of GAG contents that normalized to the value of control group were as followed: 2h group—75.1 \pm 8.2%; 4h group—64.9 \pm 7.6%; 8h group—51.3 \pm 5.8% (Fig 2A and 2B, * $p < 0.05$, *** $p < 0.001$). On the contrary, the cell viability was maintained over time. Digital image analysis showed that there were no significant differences in chondrocyte viability or viable chondrocyte density between groups (Fig 2D and 2E).

3.2 Comparison of μ CT value and GAG content in OCAs

The anionic, Iobrix contrast agent is diffused into the ECM of articular cartilage in inverse proportion to the GAG content. Further, the μ CT and histological staining analyses were performed in the same OCA. Fig 3A shows a resulting image of μ CT and histological analysis. As the chondroitinase application time increased, μ CT value (HU value) was also increased. The increase is most significant in the superficial zone of the articular cartilage tissue, whereas less noticeable in the deep zone. In the Safranin-O-stained histological sections, it can be seen that there was increased GAG degradation in the superficial zone of the tissue, and that the red staining progressively decreased. This is consistent with the results of μ CT images (Fig 3A). 64 OCAs are used to compare the μ CT values and GAG contents, including in vitro experimental samples and preliminary in vivo experimental samples. With increasing treatment time of chondroitinase, the GAG content of OCA decreases whereas the μ CT value increases (Fig 3B and 3C). The graph showed a linearly negative correlation between the CT value and the GAG content, with an R^2 value of 0.9062 (Fig 3D). The biomechanical characteristics were evaluated by detecting the compressive modulus of OCA in each group. The results showed that there were no statistically significant differences between the control group and the 2h group. By

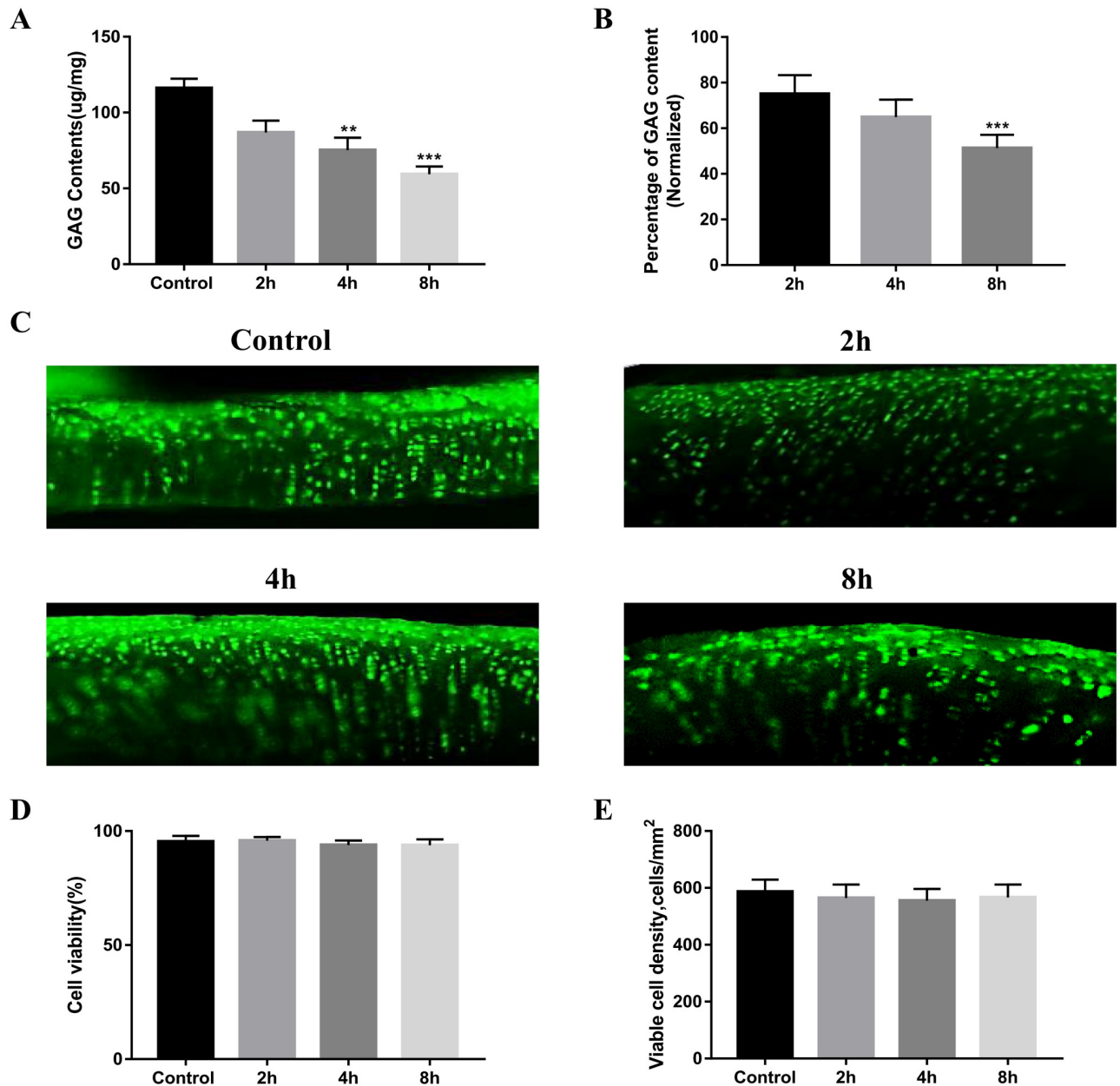


Fig 2. Changes in GAG contents and cell viability after chondroitinase treatment. A Biochemical analysis of each group of OCA GAG content and B normalized percentage (n = 10). C Live-dead Confocal microscope images of different groups of OCAs, where dead cells are stained in red and live cells are stained in green. D Quantitative analysis of cell viability and e) viable cell density of each group by Image J software (n = 4). Statistical analysis was conducted using One-way ANOVA test (*p < 0.05, **p < 0.01, ***p < 0.001). Magnification x50.

<https://doi.org/10.1371/journal.pone.0285733.g002>

contrast, the compressive modulus of both the 4h group and the 8h group were significantly lower than those of the control group (Fig 3E, *p < 0.05, ***p < 0.001). In the histological scoring results, the scores of the 4h group and the 8h group were statistically lower than those of the control group. There was no statistically significant difference between the control group and the 2h group (Fig 3F, **p < 0.01).

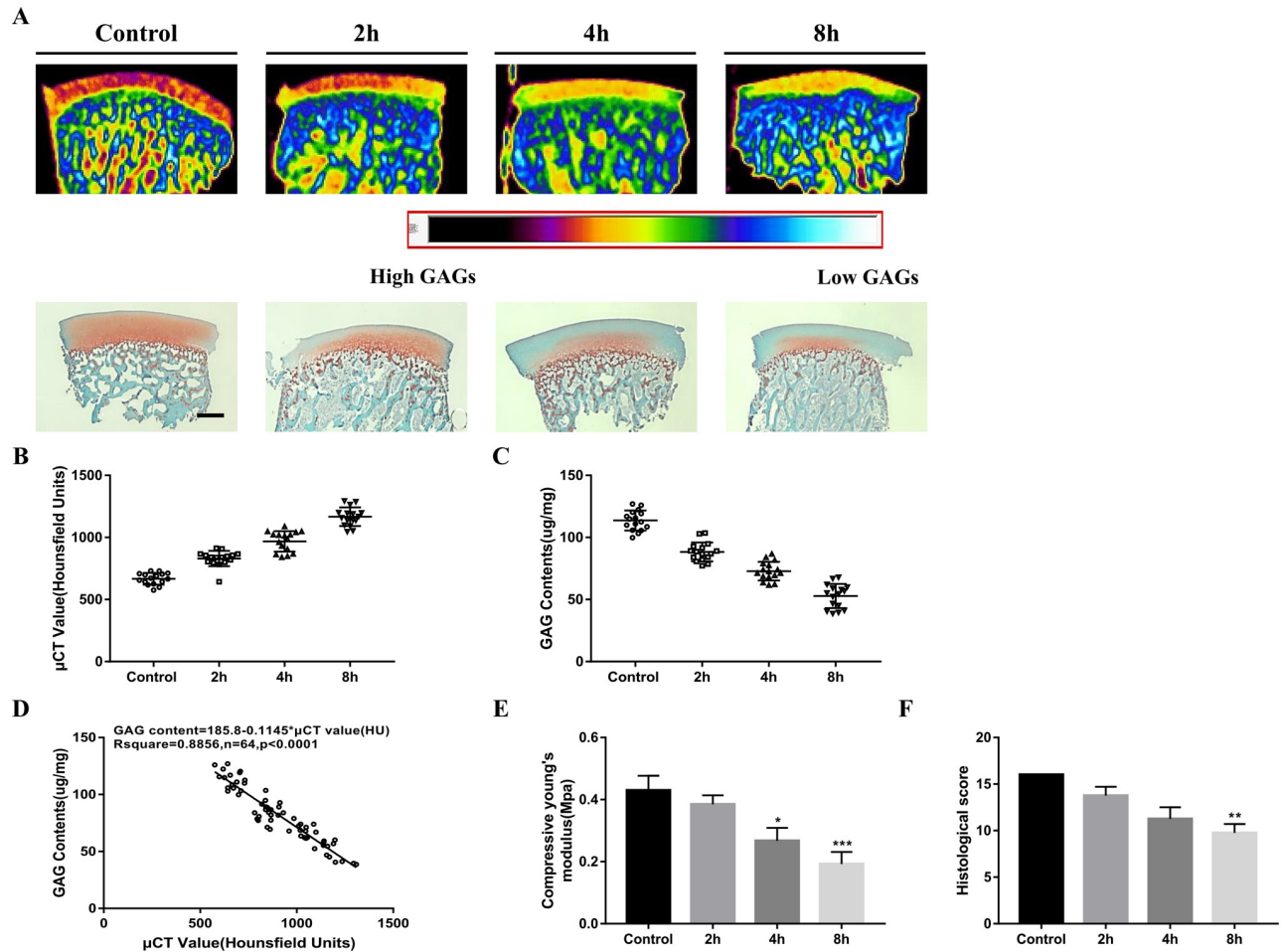


Fig 3. Changes in GAG content analysis according to μ CT analysis in OCA grafts after chondroitinase treatment. A Representative μ CT images and safranin-o-stained images of control and degraded OCA (2h, 4h, and 8h exposure to chondroitinase), the trends of the two analyzed images are inversely proportional to each other ($n = 4$). Scale bar = 500 μ m. B, C Comparison of μ CT value and GAG content of each group of OCAs (including in vitro and preliminary in vivo experimental OCAs; 64 in total). With increasing chondroitinase treatment time, the CT value of OCA increased whereas the GAG content decreased. D Linear regression plots: μ CT value vs GAG content measured by biochemical assay ($n = 64$). The R^2 in the linear regression graph is 0.8856. E Biomechanical analysis of each group after chondroitinase treatment ($n = 4$) and F histological score of OCA in each group ($n = 4$). Statistical analysis was conducted using One-way ANOVA test (* $p < 0.05$, ** $p < 0.01$, *** $p < 0.001$).

<https://doi.org/10.1371/journal.pone.0285733.g003>

3.3 Preoperative evaluation of OCAs

The preoperative quality evaluation showed that the average μ CT value for pretreatment cartilage in each group was as followed: control group—583.9 \pm 23.3 HU, 2h group—575.4 \pm 48.5 HU, 4h group—563.5 \pm 31.0 HU, 8h group—601.9 \pm 32.7 HU. Further, the GAG content was calculated based on the relationship between μ CT and GAG content: control group—118.9 \pm 2.7, 2h group—119.9 \pm 5.6, 4h group—121.3 \pm 3.6, 8h group—116.9 \pm 3.7 ug/mg. After chondroitinase treatment, the average μ CT value of each group was 846.8 \pm 18.7 HU at 2h group, 945.7 \pm 30.4 HU at 4h group, and 1089.9 \pm 22.7 HU at 8h group. The calculated GAG contents from the estimated formula were 88.8 \pm 2.1 at 2h group, 77.5 \pm 3.5 at 4h group, and 61.0 \pm 2.6 ug/mg at 8h group. The percentages of GAG content before and after treatment with chondroitinase were: 2h group—74.2 \pm 3.6%, 4h group—63.9 \pm 2.5%, 8h group—52.2 \pm 2.5% (Table 1).

Table 1. Quality assessment of OCA before animal experiment.

Group	HU (Pre-treatment)	μ CT GAG quantification	HU (Post-treatment)	μ CT GAG quantification	Percentage of GAG contents (%)
Control	583.9 \pm 23.3	118.9 \pm 2.7	-	-	-
2h	575.4 \pm 48.5	119.9 \pm 5.6	846.8 \pm 18.7	88.8 \pm 2.1	74.2 \pm 3.6%
4h	563.5 \pm 31.0	121.3 \pm 3.6	945.7 \pm 30.4	77.5 \pm 3.5	63.9 \pm 2.5%
8h	601.9 \pm 32.7	116.9 \pm 3.7	1089.9 \pm 22.7	61.0 \pm 2.6	52.2 \pm 2.5%

<https://doi.org/10.1371/journal.pone.0285733.t001>

These results are consistent with the GAG content potential measured by DMMB analysis in Fig 2.

3.4 Gross morphological evaluation of OCAs

After 4 weeks implantation, the gross morphological observation results showed that the transplantation sites in the Control group and the 2h group were filled with relatively smooth surfaces and that there was a slight gap between the graft and the host tissue. By contrast, the transplantation sites in the 4h group and 8h group were less filled than the former groups. Moreover, the surface was relatively irregular and the integration with the surrounding host cartilage was inferior to control group. After 12 weeks implantation, the transplantation sites of the Control group and the 2h group were completely repaired by the graft, appearing close to normal tissues. Also, they had a higher degree of fusion with the host tissues. However, tissue defects were still observed in the transplantation sites of the 4h group and the 8h group at 12 weeks, with irregular surfaces and tissue gaps between the host and the graft (Fig 4A). The ICRS assessment results showed that the scores of the control group and the 2h group were higher than those of the 8h group (Fig 4B, **, ## $p < 0.01$) at 4 weeks. There was no statistically significant difference with the scores of the control group and 4h group. At 12 weeks, the scores of the control group and the 2h group were higher than those of the 4h and 8h groups, with a statistical difference (***, ### $p < 0.001$). And the score of the 4h group was also higher than that of the 8h group, which was statistically significant (+++ $p < 0.001$).

3.5 Biomechanical analysis of OCAs

Biomechanical tests were performed at 4 and 12 weeks postoperatively to demonstrate the mechanical properties of the graft site. At 4 weeks, the compressive moduli of the control group and the 2h group were higher than those of the 4h and 8h groups, with a statistical difference (Fig 4C, *, # $p < 0.05$, **, ## $p < 0.01$). At 12 weeks, it was found that the compressive modulus of the control group and the 2h group was significantly higher than that of the 4h and 8h groups (***, ### $p < 0.001$), and the value of the 4h group was also higher than 8h group, with a statistical difference (+ $p < 0.05$).

3.6 Histological and μ CT evaluation of OCAs

At 4 weeks, Safranin O staining was performed to reveal cartilaginous ECM deposition in the OCA. The OCAs of the Control group and the 2h group were strongly stained by Safranin O, after which they were close to the color intensity of the surrounding normal tissues, while the staining intensities of the 4h and 8h groups were significantly reduced and very different from those of the surrounding normal tissues. At 12 weeks, the OCAs in the control and 2h groups, which seemed similar to normal cartilage, were found to completely integrate with the surrounding normal tissues. Compared to the control group, the 4h group and the 8h group had less ECM staining, irregular surface, and poor fusion with the surrounding tissue. In the 8h

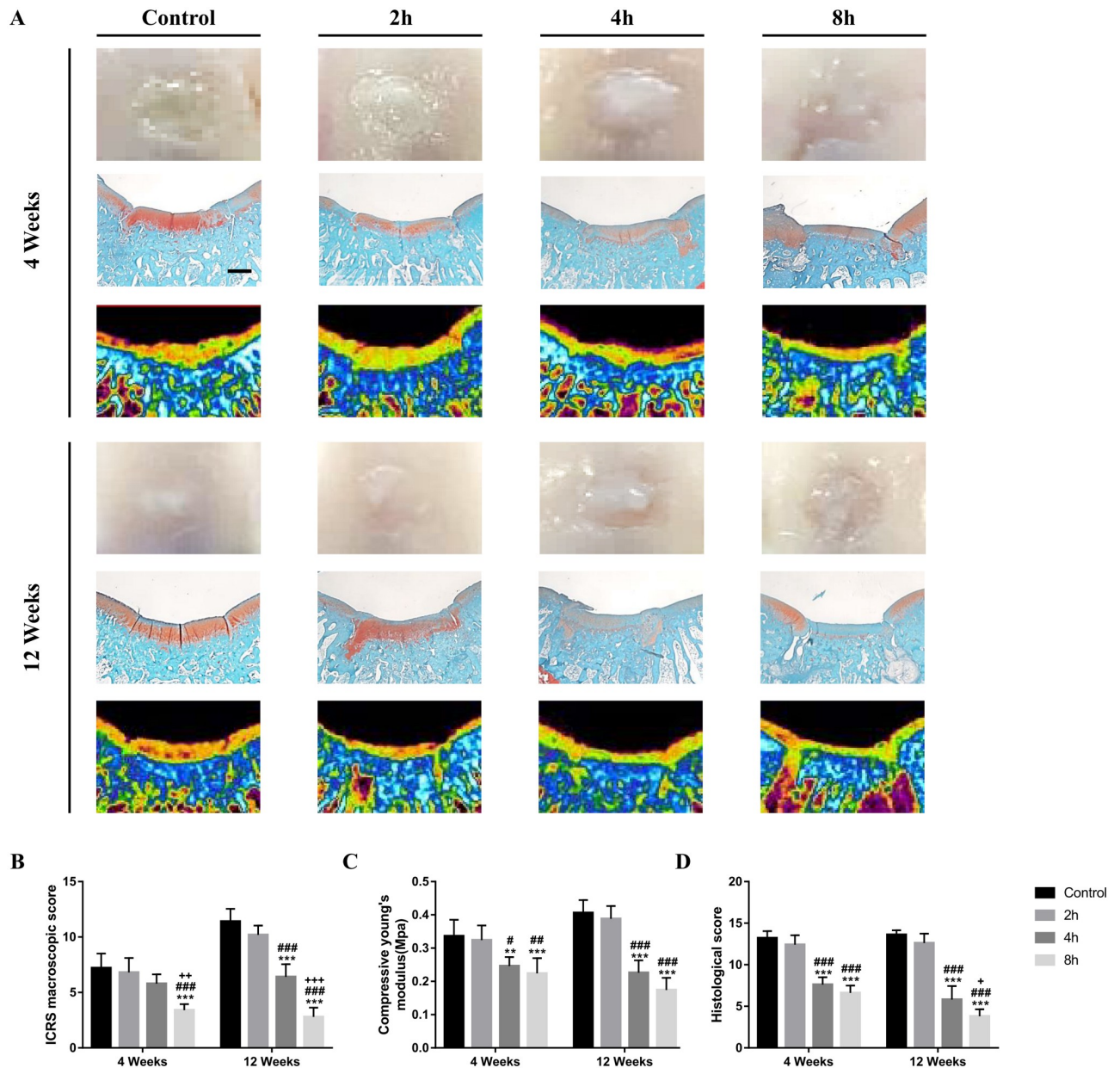


Fig 4. In vivo experimental analysis of OCA transplant sites. A Representative gross morphological image, representative Safranin-O staining (n = 5), and μ CT analysis images of the OCA transplantation site at 4 and 12 weeks postoperatively. Scale bar = 1 mm. B The scores of the International Cartilage Research Society (ICRS) macroscopic evaluation of each transplantation site. Statistical analysis was determined by Kruskal-Wallis test with Dunn's tests. C Intergroup comparison of compressive modulus was used to evaluate the biomechanical properties (n = 5). D Histological scores for the OCA transplantation site at 4 and 12 weeks after surgery (n = 5). Data represent the means \pm SD, *P < 0.05, **P < 0.01, ***P < 0.001 between control group and remaining group. #P < 0.05, ##P < 0.01, ###P < 0.001 between 2h group and remaining group. +P < 0.05, +++P < 0.001 between 4h group and 8h group. Data were analyzed by two-way ANOVA with Tukey's test if not described.

<https://doi.org/10.1371/journal.pone.0285733.g004>

group, the ECM staining at the transplantation site was severely reduced, the fusion with the surrounding tissue was poor, and tissue collapse was visible at the transplantation site. The histological scores of the control group and the 2h group were significantly higher than those of the other groups at 4 weeks and 12 weeks (Fig 4D, ***, ### p<0.001). And at 12 weeks, the 4h score was higher than the 8h score, and there was a statistical difference (+p<0.05).

Table 2. Quality assessment of OCA after animal experiment.

Time	Group	HU (Post-surgery)	μ CT GAG quantification	Percentage of GAG contents (%)
4 weeks	Control	628.0 \pm 30.1	113.9 \pm 3.4	95.8 \pm 3.7%
	2h	854.2 \pm 23.4	88.0 \pm 2.7	73.4 \pm 2.5%
	4h	1052.6 \pm 45.3	65.3 \pm 5.2	53.9 \pm 5.5%
	8h	1158.3 \pm 43.2	53.2 \pm 4.9	45.5 \pm 4.5%
12weeks	Control	621.2 \pm 35.8	114.7 \pm 4.1	96.4 \pm 3.4%
	2h	847.7 \pm 36.5	88.7 \pm 4.2	74.0 \pm 2.7%
	4h	1126.2 \pm 46.3	56.9 \pm 5.3	46.9 \pm 3.8%
	8h	1261.8 \pm 39.9	41.3 \pm 4.6	35.4 \pm 4.2%

<https://doi.org/10.1371/journal.pone.0285733.t002>

3.7 Postoperative evaluation of OCAs

The quality evaluation at 4 weeks after operation showed that the mean value of μ CT of transplanted sites in each group was: control group—628.0 \pm 30.1, 2h group—854.2 \pm 23.4, 4h group—1052.6 \pm 45.3, 8h group—1158.3 \pm 43.2 HU. The GAG contents were calculated according to the relationship between μ CT and GAG content as follows: control group—113.9 \pm 3.4, 2h group—88.0 \pm 2.7, 4h group—65.3 \pm 5.2, 8h group—53.2 \pm 4.9 ug/mg. Compared to the GAG content before chondroitinase treatment, the percentages of GAG content after treatment were as follows: control group—95.8 \pm 3.7%, 2h group—73.4 \pm 2.5%, 4h group—53.9 \pm 5.4%, 8h group—45.5 \pm 4.5%. Similarly, the mean values of μ CT at the transplantation sites in each group at 12 weeks after operation were: control group—621.2 \pm 35.8, 2h group—847.7 \pm 36.5, 4h group—1126.2 \pm 46.3, 8h group—1261.8 \pm 39.9 HU. The GAG content was calculated according to the relationship between μ CT and GAG content, with the following results obtained: control group—114.7 \pm 4.1, 2h group—88.7 \pm 4.2, 4h group—56.9 \pm 5.3, 8h group—41.3 \pm 4.6ug/mg. The percentages were as follows: control group—96.4 \pm 3.4%, 2h group—74.0 \pm 2.7%, 4h group—46.9 \pm 3.8%, 8h group—35.4 \pm 4.2% (Table 2).

3.8 Evaluation of functional changes in postoperative OCAs

The estimation of GAG contents using μ CT imaging, histological and biomechanical analysis of OCA at the transplantation site was performed at 4 and 12 weeks after surgery to verify the effect of OCAs possessing different GAG contents on the functional regeneration of cartilage (Fig 5). The estimated GAG contents by μ CT analysis showed that there was no significant change in GAG content in the control and 2h groups at 4 and 12 weeks, while the GAG content at 12 weeks in the 4h and 8h groups was lower than that at 4 weeks (Fig 5A, * p <0.05, *** p <0.001). The results of Safranin-O staining showed that there was no significant difference in histological scores between the control group and the 2h group, while the scores at 12 weeks were lower than those at 4 weeks in the 4h and 8h groups (Fig 5B, ** p <0.01, *** p <0.001). Biomechanical results showed that the compressive modulus at 12 weeks was higher than that at 4 weeks in the control and 2h groups, whereas in the 8h group, the compressive modulus at 4 weeks was higher than that at 12 weeks (Fig 5C, * p <0.05).

3.9 Cell viability and percentage of viable cells of OCAs

At 12 weeks after surgery, the cell viability and viable cell density at the transplantation site were evaluated by live/dead staining. Dead cells were hardly observed in the live/dead stained images of the Control and 2h groups. By contrast, more dead cells were observed in the images of the 4h and 8h groups, mainly in the cartilage superficial zone. In the 8h group in particular,

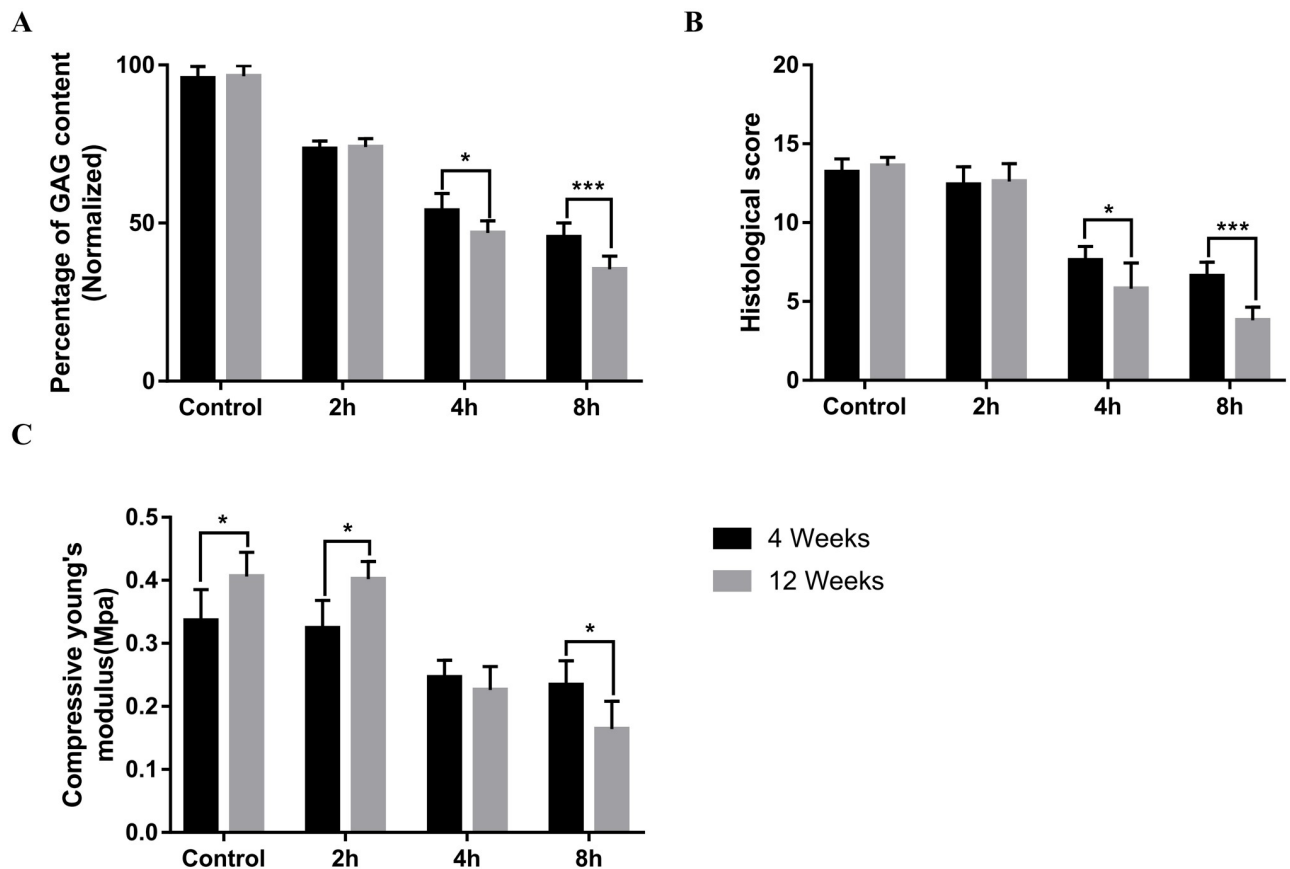


Fig 5. Changes in OCA effect after 4 and 12 weeks of transplantation. A Quantification of GAG content at the graft site by μ CT analysis, B histological score and C compressive modulus were compared at 4 and 12 weeks postoperatively (* $p < 0.05$ ** $p < 0.01$, *** $p < 0.001$).

<https://doi.org/10.1371/journal.pone.0285733.g005>

dead cells were observed in the middle zone (Fig 6A). Quantitative analysis was used to compare the cell viability and viable cell density. The average cell viabilities in the control group and the 2h group were 93% and 88%, with no significant difference. By contrast, the cell viabilities in the 4h and 8h groups were 55% and 33%, respectively, with a significant downward trend, particularly in the 8h group (Fig 6B, $p < 0.001$). The same trend was observed in the quantitative analysis of the viable cell density results (Fig 6C, $p < 0.001$).

4 Discussion

The current study evaluated the efficacy of GAG content in OCA. The Control, 2h, 4h, and 8h groups were set based on the different treatment times of graft chondroitinase. We found that the functional effects of OCA were reduced in the 4h and 8h groups compared to in the control and 2h groups, thus leading to OCA functional failure. Further, the comparison between 4 and 12 weeks after surgery showed that the GAG contents, biomechanical characteristics, and histological scores of the transplanted sites in the control and 2h groups were better maintained than those in the 4h and 8h groups. Therefore, the GAG content of the graft has the potential to be a key factor in assessing the functional success of OCA.

Hyaline cartilage is a load-bearing tissue that supports joints and evenly distributes mechanical loads. Further, because GAG is made up of polysaccharide chains and has a high

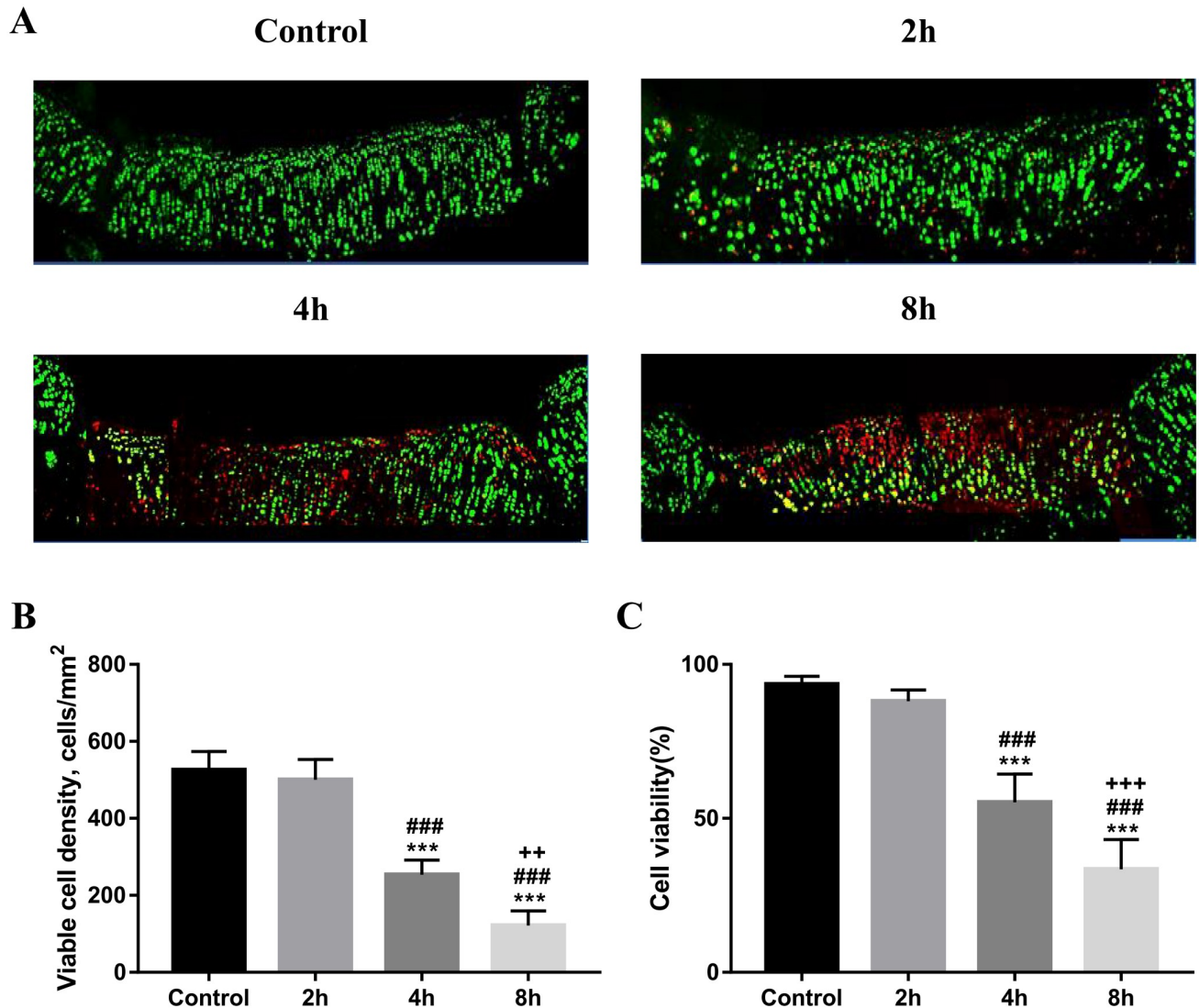


Fig 6. Cell viability at the OCA transplantation site at 12 weeks postoperative (n = 5). A Representative live/dead stained images of the OCA transplantation sites at 12 weeks after surgery. Dead cells are marked in red whereas live cells are marked in green. B Percentage of cell viability in transplantation site. C Quantitative analysis of the available cell density in the transplantation site (* $p < 0.05$, ** $p < 0.01$, *** $p < 0.001$). Magnification $\times 20$.

<https://doi.org/10.1371/journal.pone.0285733.g006>

negative charge and strong hydrophilicity, it draws osmotically active Na^+ , which causes a significant amount of water to be drawn into its structure. Based on the effects of osmotic pressure and chemical expansion stress caused by these GAG characteristics, the ECM can endure compressive forces [47]. When cartilage tissue is subjected to continuous pressure load, this function maintains the stability of the extracellular microenvironment, which ultimately prevents cell damage and cell apoptosis [34, 35, 37]. Levin A.S. et al. [48] proved that the GAG content in immature bovine cartilage was higher than that in mature bovine cartilage, and that the cells in the former are less vulnerable to load-induced injury. Otsuki S. et al. [40] proved that GAG loss alone did not directly lead to chondrocyte death. In response to mechanical injury, there is an immediate induction of necrotic cell death. Similarly, in our histological analysis, as the GAG content of the graft decreased (from the control group to the 8h group),

the remodeling ability and histological score of the graft site decreased at both 4 and 12 weeks postoperatively (Fig 4A and 4D). The results of the biomechanical analysis showed that the compressive moduli of the control group and the 2h group were higher than those of the 4h and 8h groups at 4 and 12 weeks after surgery, indicating that the GAG content of the graft would affect the postoperative biomechanical properties (Fig 4C). Further, in the 4h and 8h groups, as the GAG content of the graft decreased, the cell viability of the graft site decreased at 12 weeks after surgery. By contrast, in both the control group and the 2h group, the cell viability of the transplanted site remained at a high level 12 weeks after the operation (Fig 6). Therefore, we assumed that changes in graft GAG content were a key factor affecting the functional success of OCA.

It is known that GAG concentrations in cartilage decrease with age. Previous study reported that human articular cartilage was obtained postmortem from the lateral femoral condyle of 30 subjects aged 1 to 70 years, and their cartilage GAG concentrations were compared. The results showed that the GAG contents of donors older than 60 years were significantly decreased [49]. In early OA, GAG in ECM will be reduced, and this decrease in GAG content reduced the elasticity of articular cartilage to compressive loads [50]. In this study, we used chondroitinase to manufacture grafts with different GAG contents, and the differences in GAG contents and the unchanged chondrocyte viability of the grafts were demonstrated by biochemical, μ CT, and cell viability analyses (Figs 2 and 3). In the *in vivo* study, the study period included 4 weeks of early follow-up and 12 weeks of late follow-up. Due to the high potential for spontaneous healing in the rabbit animal model, the functional effects of each group of OCA were assessed at 4 weeks postoperatively [51, 52]. Shapiro et al. demonstrated encouraging results for 3mm osteochondral defect in rabbit model, at 12 weeks postoperatively [53]. We compared the functional effects of OCA at 4 and 12 weeks postoperatively by imaging, histological, and biomechanical analyses. In the quantitative analysis of μ CT, the GAG content in the 4h and 8h groups decreased significantly from 4 weeks to 12 weeks after surgery, which was the same trend as the Safranin-O staining score (Fig 5A and 5B). And in the biomechanical analysis, with the increase of follow-up time, the compressive modulus of the 8h group decreased significantly (Fig 5C). These results further demonstrated that GAG content in OCA might play an important role in osteochondral repair.

GAG in articular cartilage ECM is a strongly hydrophilic polymer composed of polysaccharide chains and is highly negatively charged [47, 54, 55]. Applying these characteristics of GAG, quantitative computed tomography (QCT) has been used to measure the concentration and spatial distribution of anionic iodine contrast agents diffused into isolated articular cartilage explants. It has also been demonstrated in various animal and human models that the μ CT value is linearly correlated with the GAG content of articular cartilage [38, 41–43]. In this study, we compared the μ CT image and Safranin-O-stained image of the same sample, and the results showed that the trend of the change in GAG content was the same (Fig 3A). Subsequently, we used μ CT analysis and biochemical analysis to measure the GAG content of each group of OCA in both *in vivo* and *in vitro* experiments (including OCA obtained at 4 and 12 weeks after surgery) and evaluated the relationship between the two analysis methods. The results show that the μ CT value of the graft is negatively correlated with the GAG content and $R^2 = 0.91$, which has a reliable value (Fig 3D). Further, after μ CT analysis, the cell viability of each group of grafts was shown to remain above 95%, which further demonstrated the feasibility of this method (Fig 2C–2E). Therefore, the results indicated that the μ CT non-destructive analysis method can be used to detect the content of GAG in cartilage tissues under various conditions, including normal cartilage and degenerated cartilage, which has high reliability and can be applied to the evaluation method of preoperative graft.

In the transplantation of other human tissues, the content of the extracellular matrix of the graft is an important factor, as is the reconstruction of tendons and ligaments. Several studies examining animal models of ACL allografts have shown that myofibroblasts in the grafts exert contractile forces through the extracellular matrix to directly affect the remodeling capacity of their grafts [56, 57]. The extracellular matrix in the tendon and ligament varies by function, thereby providing appropriate mechanical properties [58]. Further, using extracellular matrix grafts to reconstruct the Achilles tendon was shown to enhance Achilles tendon repair, reduce gaps, and improve biomechanical effects [59, 60]. Therefore, ECM is an important influencing factor in grafts, and our study found that GAG can affect the functional effect of OCA and may become an important biomarker.

In this study, chondroitinase ABC was used to create graft models containing different concentrations of GAG. Chondroitinase ABC is a GAG-specific hydrolase that is used to digest chondroitin sulfate in proteoglycan complexes. Previous studies have shown that it can specifically degrade the content of GAG in tissues while having little effect on other components such as collagen [61, 62]. Chondroitinase has been used in many studies to modulate GAG concentrations, including in vitro and in vivo experiments in various animal and human models. Further, the change in the treatment conditions of chondroitinase can obtain more cartilage models with different GAG contents and simultaneously little effect on chondrocytes during the treatment [40, 62, 63]. We used 1 Unit/ml concentration of chondroitinase to create three transplantation models with different GAG concentrations under different treatment time conditions. The grafts in each group were treated with chondroitinase, rinsed three times with PBS solution, and then subjected to live/dead staining experiments. The results showed that few dead cells were observed in the cartilage tissue of each group, the cell survival rate was above 95%, and the difference between the groups was not statistically significant. This indicated that the chondroitinase treatment process had less effect on tissue cell viability, which is consistent with the previous findings.

This study has the following limitations: The first limitation is the selection of experimental animals. In this study, a rabbit model was used for in vivo research. The rabbit model possessed several limitations such as self-regenerative capacity, thinner cartilage thickness, and small defect area. Secondly, we measured GAG content before and after OCA surgery by μ CT noninvasive analysis method. Although the test results showed that its confidential range was high, the μ CT value is an indirect quantification of GAG content which may be slightly different from its own content. Finally, we manufactured grafts with different GAG content by using chondroitinase and evaluated the effect of GAG content on the functional efficacy of OCA. However, the method of making a graft model by using chondroitinase is fundamentally different than the actual difference between donors, because differences between donors are generated under important factors such as age, BMI, and history of trauma. Therefore, it is necessary to further analyze the changes in GAG contents in human donor grafts, which could be the content of our follow-up study.

In conclusion, reduced GAG contents of grafts in the rabbit model were found to affect the functional effects of post-transplantation OCA. In this study, non-destructive analysis of μ CT was conducted to evaluate the GAG content of the graft before and after surgery and to verify the effectiveness of the method. Altogether, the results indicated that this quality analysis method for the preoperative evaluation of grafts could be applied in clinical treatment.

Supporting information

S1 Fig. Rabbit animal model of osteochondral allograft transplantation. (A) Graft harvested from a donor rabbit knee trochlea. (B) The size of the graft is 4 mm in diameter and 2.5 mm in

depth. (C) Fully exposed recipient rabbit knee pulley. (D) Finally, the picture after implantation of the osteochondral graft.
(TIF)

Author Contributions

Conceptualization: Do Young Park, Dong Il Shin, Jin Ho Park, Byoung-Hyun Min.

Data curation: Yong Jun Jin, Sujin Noh, Jin Ho Park.

Formal analysis: Yong Jun Jin, HyeonJae Kwon, Dong Il Shin.

Funding acquisition: Byoung-Hyun Min.

Investigation: Yong Jun Jin, HyeonJae Kwon.

Methodology: Yong Jun Jin, Sujin Noh, HyeonJae Kwon, Dong Il Shin, Jin Ho Park.

Project administration: Sujin Noh, Byoung-Hyun Min.

Resources: HyeonJae Kwon.

Software: Yong Jun Jin, Sujin Noh, HyeonJae Kwon, Jin Ho Park.

Supervision: Do Young Park, Sujin Noh, Byoung-Hyun Min.

Validation: Yong Jun Jin, Do Young Park, Dong Il Shin.

Visualization: Yong Jun Jin.

Writing – original draft: Yong Jun Jin.

Writing – review & editing: Do Young Park, Byoung-Hyun Min.

References

1. Curl WW, Krome J, Gordon ES, Rushing J, Smith BP, Poehling GG. Cartilage injuries: a review of 31,516 knee arthroscopies. *Arthroscopy*. 1997; 13(4):456–60. Epub 1997/08/01. [https://doi.org/10.1016/s0749-8063\(97\)90124-9](https://doi.org/10.1016/s0749-8063(97)90124-9) PMID: 9276052.
2. Spahn G, Kahl E, Muckley T, Hofmann GO, Klinger HM. Arthroscopic knee chondroplasty using a bipolar radiofrequency-based device compared to mechanical shaver: results of a prospective, randomized, controlled study. *Knee Surg Sports Traumatol Arthrosc*. 2008; 16(6):565–73. Epub 2008/03/11. <https://doi.org/10.1007/s00167-008-0506-1> PMID: 18327566.
3. O'Driscoll SW. The healing and regeneration of articular cartilage. *J Bone Joint Surg Am*. 1998; 80(12):1795–812. Epub 1999/01/06. PMID: 9875939.
4. Frisbie DD, Oxford JT, Southwood L, Trotter GW, Rodkey WG, Steadman JR, et al. Early events in cartilage repair after subchondral bone microfracture. *Clin Orthop Relat Res*. 2003;(407):215–27. Epub 2003/02/05. <https://doi.org/10.1097/00003086-200302000-00031> PMID: 12567150.
5. Bedi A, Feeley BT, Williams RJ 3rd. Management of articular cartilage defects of the knee. *J Bone Joint Surg Am*. 2010; 92(4):994–1009. Epub 2010/04/03. <https://doi.org/10.2106/JBJS.I.00895> PMID: 20360528.
6. Davis DD, Kane SM. Cartilage Graft. *StatPearls*. Treasure Island (FL)2021.
7. Frank RM, Lee S, Levy D, Poland S, Smith M, Scalise N, et al. Osteochondral Allograft Transplantation of the Knee: Analysis of Failures at 5 Years. *Am J Sports Med*. 2017; 45(4):864–74. Epub 2017/01/07. <https://doi.org/10.1177/0363546516676072> PMID: 28056527.
8. Krych AJ, Saris DBF, Stuart MJ, Hacken B. Cartilage Injury in the Knee: Assessment and Treatment Options. *J Am Acad Orthop Surg*. 2020; 28(22):914–22. Epub 2020/08/17. <https://doi.org/10.5435/JAAOS-D-20-00266> PMID: 32796370.
9. Du D, Hsu P, Zhu Z, Zhang C. Current surgical options and innovation for repairing articular cartilage defects in the femoral head. *J Orthop Translat*. 2020; 21:122–8. Epub 2020/04/21. <https://doi.org/10.1016/j.jot.2019.06.002> PMID: 32309137.

10. Emmerson BC, Gortz S, Jamali AA, Chung C, Amiel D, Bugbee WD. Fresh osteochondral allografting in the treatment of osteochondritis dissecans of the femoral condyle. *Am J Sports Med.* 2007; 35(6):907–14. Epub 2007/03/21. <https://doi.org/10.1177/0363546507299932> PMID: 17369560.
11. Gilat R, Haunschild ED, Huddleston HP, Tauro TM, Patel S, Wolfson TS, et al. Osteochondral Allograft Transplant for Focal Cartilage Defects of the Femoral Condyles: Clinically Significant Outcomes, Failures, and Survival at a Minimum 5-Year Follow-up. *Am J Sports Med.* 2021; 49(2):467–75. Epub 2021/01/12. <https://doi.org/10.1177/0363546520980087> PMID: 33428427.
12. Chahal J, Gross AE, Gross C, Mall N, Dwyer T, Chahal A, et al. Outcomes of osteochondral allograft transplantation in the knee. *Arthroscopy.* 2013; 29(3):575–88. Epub 2013/04/03. <https://doi.org/10.1016/j.arthro.2012.12.002> PMID: 23544690.
13. Cook JL, Stannard JP, Stoker AM, Bozynski CC, Kuroki K, Cook CR, et al. Importance of Donor Chondrocyte Viability for Osteochondral Allografts. *Am J Sports Med.* 2016; 44(5):1260–8. Epub 2016/02/28. <https://doi.org/10.1177/0363546516629434> PMID: 26920431.
14. Farr J, Gomoll AH. 2016 barriers to cartilage restoration. *J Clin Orthop Trauma.* 2016; 7(3):183–6. Epub 2016/08/05. <https://doi.org/10.1016/j.jcot.2016.05.001> PMID: 27489414.
15. Williams SK, Amiel D, Ball ST, Allen RT, Wong VW, Chen AC, et al. Prolonged storage effects on the articular cartilage of fresh human osteochondral allografts. *J Bone Joint Surg Am.* 2003; 85(11):2111–20. Epub 2003/11/25. <https://doi.org/10.2106/00004623-200311000-00008> PMID: 14630839.
16. Bugbee WD, Pallante-Kichura AL, Gortz S, Amiel D, Sah R. Osteochondral allograft transplantation in cartilage repair: Graft storage paradigm, translational models, and clinical applications. *J Orthop Res.* 2016; 34(1):31–8. Epub 2015/08/04. <https://doi.org/10.1002/jor.22998> PMID: 26234194.
17. Malinin T, Temple HT, Buck BE. Transplantation of osteochondral allografts after cold storage. *J Bone Joint Surg Am.* 2006; 88(4):762–70. Epub 2006/04/06. PMID: 16595466.
18. Gross AE, Kim W, Las Heras F, Backstein D, Safir O, Pritzker KP. Fresh osteochondral allografts for posttraumatic knee defects: long-term followup. *Clin Orthop Relat Res.* 2008; 466(8):1863–70. Epub 2008/05/10. <https://doi.org/10.1007/s11999-008-0282-8> PMID: 18465182.
19. Williams SK, Amiel D, Ball ST, Allen RT, Tontz WL Jr., Emmerson BC, et al. Analysis of cartilage tissue on a cellular level in fresh osteochondral allograft retrievals. *Am J Sports Med.* 2007; 35(12):2022–32. Epub 2007/08/29. <https://doi.org/10.1177/0363546507305017> PMID: 17724095.
20. Hangody LR, Gal T, Szucs A, Vasarhelyi G, Toth F, Modis L, et al. Osteochondral allograft transplantation from a living donor. *Arthroscopy.* 2012; 28(8):1180–3. Epub 2012/07/31. <https://doi.org/10.1016/j.arthro.2012.05.880> PMID: 22840989.
21. Jomha NM, Elliott JA, Law GK, Maghdoori B, Forbes JF, Abazari A, et al. Vitrification of intact human articular cartilage. *Biomaterials.* 2012; 33(26):6061–8. Epub 2012/06/16. <https://doi.org/10.1016/j.biomaterials.2012.05.007> PMID: 22698720.
22. Stoker AM, Stannard JP, Kuroki K, Bozynski CC, Pfeiffer FM, Cook JL. Validation of the Missouri Osteochondral Allograft Preservation System for the Maintenance of Osteochondral Allograft Quality During Prolonged Storage. *Am J Sports Med.* 2018; 46(1):58–65. Epub 2017/09/25. <https://doi.org/10.1177/0363546517727516> PMID: 28937783.
23. Rosa SC, Goncalves J, Judas F, Lopes C, Mendes AF. Assessment of strategies to increase chondrocyte viability in cryopreserved human osteochondral allografts: evaluation of the glycosylated hydroquinone, arbutin. *Osteoarthritis Cartilage.* 2009; 17(12):1657–61. Epub 2009/09/16. <https://doi.org/10.1016/j.joca.2009.08.016> PMID: 19751692.
24. Guilak F, Alexopoulos LG, Upton ML, Youn I, Choi JB, Cao L, et al. The pericellular matrix as a transducer of biomechanical and biochemical signals in articular cartilage. *Ann N Y Acad Sci.* 2006; 1068:498–512. Epub 2006/07/13. <https://doi.org/10.1196/annals.1346.011> PMID: 16831947.
25. Sutherland AJ, Converse GL, Hopkins RA, Detamore MS. The bioactivity of cartilage extracellular matrix in articular cartilage regeneration. *Adv Healthc Mater.* 2015; 4(1):29–39. Epub 2014/07/22. <https://doi.org/10.1002/adhm.201400165> PMID: 25044502.
26. Chandrasekhar S, Harvey AK. Induction of interleukin-1 receptors on chondrocytes by fibroblast growth factor: a possible mechanism for modulation of interleukin-1 activity. *J Cell Physiol.* 1989; 138(2):236–46. Epub 1989/02/01. <https://doi.org/10.1002/jcp.1041380204> PMID: 2537323.
27. Verschure PJ, van Marle J, Joosten LA, van den Berg WB. Chondrocyte IGF-1 receptor expression and responsiveness to IGF-1 stimulation in mouse articular cartilage during various phases of experimentally induced arthritis. *Ann Rheum Dis.* 1995; 54(8):645–53. Epub 1995/08/01. <https://doi.org/10.1136/ard.54.8.645> PMID: 7677441.
28. Wang J, Verdonk P, Elewaut D, Veys EM, Verbruggen G. Homeostasis of the extracellular matrix of normal and osteoarthritic human articular cartilage chondrocytes in vitro. *Osteoarthritis Cartilage.* 2003; 11(11):801–9. Epub 2003/11/12. [https://doi.org/10.1016/s1063-4584\(03\)00168-7](https://doi.org/10.1016/s1063-4584(03)00168-7) PMID: 14609533.

29. Benders KE, van Weeren PR, Badylak SF, Saris DB, Dhert WJ, Malda J. Extracellular matrix scaffolds for cartilage and bone regeneration. *Trends Biotechnol.* 2013; 31(3):169–76. Epub 2013/01/10. <https://doi.org/10.1016/j.tibtech.2012.12.004> PMID: 23298610.
30. Peng Z, Sun H, Bunpetch V, Koh Y, Wen Y, Wu D, et al. The regulation of cartilage extracellular matrix homeostasis in joint cartilage degeneration and regeneration. *Biomaterials.* 2021; 268:120555. Epub 2020/12/08. <https://doi.org/10.1016/j.biomaterials.2020.120555> PMID: 33285440.
31. Theocharis AD, Skandalis SS, Gialeli C, Karamanos NK. Extracellular matrix structure. *Adv Drug Deliv Rev.* 2016; 97:4–27. Epub 2015/11/13. <https://doi.org/10.1016/j.addr.2015.11.001> PMID: 26562801.
32. Sacitharan PK. Ageing and Osteoarthritis. *Subcell Biochem.* 2019; 91:123–59. Epub 2019/03/20. https://doi.org/10.1007/978-981-13-3681-2_6 PMID: 30888652.
33. Buckwalter JA, Mankin HJ, Grodzinsky AJ. Articular cartilage and osteoarthritis. *Instr Course Lect.* 2005; 54:465–80. Epub 2005/06/15. PMID: 15952258.
34. Vrana NE, Hasirci V, McGuinness GB, Ndreu-Hallil A. Cell/tissue microenvironment engineering and monitoring in tissue engineering, regenerative medicine, and in vitro tissue models. *Biomed Res Int.* 2014; 2014:951626. Epub 2014/09/24. <https://doi.org/10.1155/2014/951626> PMID: 25247195.
35. Choi JB, Youn I, Cao L, Leddy HA, Gilchrist CL, Setton LA, et al. Zonal changes in the three-dimensional morphology of the chondron under compression: the relationship among cellular, pericellular, and extracellular deformation in articular cartilage. *J Biomech.* 2007; 40(12):2596–603. Epub 2007/04/03. <https://doi.org/10.1016/j.jbiomech.2007.01.009> PMID: 17397851.
36. Poole CA, Flint MH, Beaumont BW. Chondrons in cartilage: ultrastructural analysis of the pericellular microenvironment in adult human articular cartilages. *J Orthop Res.* 1987; 5(4):509–22. Epub 1987/01/01. <https://doi.org/10.1002/jor.1100050406> PMID: 3681525.
37. Athanasiou KA, Rosenwasser MP, Buckwalter JA, Malinin TI, Mow VC. Interspecies comparisons of in situ intrinsic mechanical properties of distal femoral cartilage. *J Orthop Res.* 1991; 9(3):330–40. Epub 1991/05/01. <https://doi.org/10.1002/jor.1100090304> PMID: 2010837.
38. Bansal PN, Joshi NS, Entezari V, Grinstaff MW, Snyder BD. Contrast enhanced computed tomography can predict the glycosaminoglycan content and biomechanical properties of articular cartilage. *Osteoarthritis Cartilage.* 2010; 18(2):184–91. Epub 2009/10/10. <https://doi.org/10.1016/j.joca.2009.09.003> PMID: 19815108.
39. D'Lima DD, Hashimoto S, Chen PC, Colwell CW Jr., Lotz MK. Human chondrocyte apoptosis in response to mechanical injury. *Osteoarthritis Cartilage.* 2001; 9(8):712–9. Epub 2002/02/14. <https://doi.org/10.1053/joca.2001.0468> PMID: 11795990.
40. Otsuki S, Brinson DC, Creighton L, Kinoshita M, Sah RL, D'Lima D, et al. The effect of glycosaminoglycan loss on chondrocyte viability: a study on porcine cartilage explants. *Arthritis Rheum.* 2008; 58(4):1076–85. Epub 2008/04/03. <https://doi.org/10.1002/art.23381> PMID: 18383360.
41. Kallioniemi AS, Jurvelin JS, Nieminen MT, Lammi MJ, Toyras J. Contrast agent enhanced pQCT of articular cartilage. *Phys Med Biol.* 2007; 52(4):1209–19. Epub 2007/02/01. <https://doi.org/10.1088/0031-9155/52/4/024> PMID: 17264381.
42. Palmer AW, Guldberg RE, Levenston ME. Analysis of cartilage matrix fixed charge density and three-dimensional morphology via contrast-enhanced microcomputed tomography. *Proc Natl Acad Sci U S A.* 2006; 103(51):19255–60. Epub 2006/12/13. <https://doi.org/10.1073/pnas.0606406103> PMID: 17158799.
43. Siebelt M, van Tiel J, Waarsing JH, Pijpers TM, van Straten M, Booij R, et al. Clinically applied CT arthrography to measure the sulphated glycosaminoglycan content of cartilage. *Osteoarthritis Cartilage.* 2011; 19(10):1183–9. Epub 2011/08/09. <https://doi.org/10.1016/j.joca.2011.07.006> PMID: 21820067.
44. Yin H, Wang Y, Sun X, Cui G, Sun Z, Chen P, et al. Functional tissue-engineered microtissue derived from cartilage extracellular matrix for articular cartilage regeneration. *Acta Biomater.* 2018; 77:127–41. Epub 2018/07/22. <https://doi.org/10.1016/j.actbio.2018.07.031> PMID: 30030172.
45. Kerin AJ, Wisnom MR, Adams MA. The compressive strength of articular cartilage. *Proc Inst Mech Eng H.* 1998; 212(4):273–80. Epub 1998/10/14. <https://doi.org/10.1243/0954411981534051> PMID: 9769695.
46. Williams RJ 3rd, Ranawat AS, Potter HG, Carter T, Warren RF. Fresh stored allografts for the treatment of osteochondral defects of the knee. *J Bone Joint Surg Am.* 2007; 89(4):718–26. Epub 2007/04/04. <https://doi.org/10.2106/JBJS.F.00625> PMID: 17403792.
47. Roughley PJ, Lee ER. Cartilage proteoglycans: structure and potential functions. *Microsc Res Tech.* 1994; 28(5):385–97. Epub 1994/08/01. <https://doi.org/10.1002/jemt.1070280505> PMID: 7919526.
48. Levin AS, Chen CT, Torzilli PA. Effect of tissue maturity on cell viability in load-injured articular cartilage explants. *Osteoarthritis Cartilage.* 2005; 13(6):488–96. Epub 2005/06/01. <https://doi.org/10.1016/j.joca.2005.01.006> PMID: 15922183.

49. Elliott RJ, Gardner DL. Changes with age in the glycosaminoglycans of human articular cartilage. *Ann Rheum Dis.* 1979; 38(4):371–7. Epub 1979/08/01. <https://doi.org/10.1136/ard.38.4.371> PMID: 496451.
50. Grushko G, Schneiderman R, Maroudas A. Some biochemical and biophysical parameters for the study of the pathogenesis of osteoarthritis: a comparison between the processes of ageing and degeneration in human hip cartilage. *Connect Tissue Res.* 1989; 19(2–4):149–76. Epub 1989/01/01. <https://doi.org/10.3109/03008208909043895> PMID: 2805680.
51. Moran CJ, Ramesh A, Brama PA, O'Byrne JM, O'Brien FJ, Levingstone TJ. The benefits and limitations of animal models for translational research in cartilage repair. *J Exp Orthop.* 2016; 3(1):1. Epub 2016/02/26. <https://doi.org/10.1186/s40634-015-0037-x> PMID: 26915001.
52. Sohn JY, Park JC, Um YJ, Jung UW, Kim CS, Cho KS, et al. Spontaneous healing capacity of rabbit cranial defects of various sizes. *J Periodontal Implant Sci.* 2010; 40(4):180–7. Epub 2010/09/10. <https://doi.org/10.5051/jpis.2010.40.4.180> PMID: 20827327.
53. Shapiro F, Koide S, Glimcher MJ. Cell origin and differentiation in the repair of full-thickness defects of articular cartilage. *J Bone Joint Surg Am.* 1993; 75(4):532–53. Epub 1993/04/01. <https://doi.org/10.2106/00004623-199304000-00009> PMID: 8478382.
54. Mow VC, Kuei SC, Lai WM, Armstrong CG. Biphasic creep and stress relaxation of articular cartilage in compression? Theory and experiments. *J Biomech Eng.* 1980; 102(1):73–84. Epub 1980/02/01. <https://doi.org/10.1115/1.3138202> PMID: 7382457.
55. Gentili C, Cancedda R. Cartilage and bone extracellular matrix. *Curr Pharm Des.* 2009; 15(12):1334–48. Epub 2009/04/10. PMID: 19355972.
56. Dustmann M, Schmidt T, Gangey I, Unterhauser FN, Weiler A, Scheffler SU. The extracellular remodeling of free-soft-tissue autografts and allografts for reconstruction of the anterior cruciate ligament: a comparison study in a sheep model. *Knee Surg Sports Traumatol Arthrosc.* 2008; 16(4):360–9. Epub 2008/01/10. <https://doi.org/10.1007/s00167-007-0471-0> PMID: 18183370.
57. Weiler A, Unterhauser FN, Bail HJ, Huning M, Haas NP. Alpha-smooth muscle actin is expressed by fibroblastic cells of the ovine anterior cruciate ligament and its free tendon graft during remodeling. *J Orthop Res.* 2002; 20(2):310–7. Epub 2002/03/29. [https://doi.org/10.1016/S0736-0266\(01\)00109-7](https://doi.org/10.1016/S0736-0266(01)00109-7) PMID: 11918311.
58. Birch HL, Thorpe CT, Rumian AP. Specialisation of extracellular matrix for function in tendons and ligaments. *Muscles Ligaments Tendons J.* 2013; 3(1):12–22. Epub 2013/07/26. <https://doi.org/10.11138/mltj/2013.3.1.012> PMID: 23885341.
59. Linn FC, Sokoloff L. Movement and Composition of Interstitial Fluid of Cartilage. *Arthritis Rheum.* 1965; 8:481–94. Epub 1965/08/01. <https://doi.org/10.1002/art.1780080402> PMID: 14323537.
60. Magnussen RA, Glisson RR, Moorman CT 3rd. Augmentation of Achilles tendon repair with extracellular matrix xenograft: a biomechanical analysis. *Am J Sports Med.* 2011; 39(7):1522–7. Epub 2011/03/05. <https://doi.org/10.1177/0363546510397815> PMID: 21372317.
61. Asanbaeva A, Masuda K, Thonar EJ, Klisch SM, Sah RL. Mechanisms of cartilage growth: modulation of balance between proteoglycan and collagen in vitro using chondroitinase ABC. *Arthritis Rheum.* 2007; 56(1):188–98. Epub 2006/12/30. <https://doi.org/10.1002/art.22298> PMID: 17195221.
62. Chen CT, Fishbein KW, Torzilli PA, Hilger A, Spencer RG, Horton WE Jr. Matrix fixed-charge density as determined by magnetic resonance microscopy of bioreactor-derived hyaline cartilage correlates with biochemical and biomechanical properties. *Arthritis Rheum.* 2003; 48(4):1047–56. Epub 2003/04/11. <https://doi.org/10.1002/art.10991> PMID: 12687548.
63. Bayliss MT, Osborne D, Woodhouse S, Davidson C. Sulfation of chondroitin sulfate in human articular cartilage. The effect of age, topographical position, and zone of cartilage on tissue composition. *J Biol Chem.* 1999; 274(22):15892–900. Epub 1999/05/21. <https://doi.org/10.1074/jbc.274.22.15892> PMID: 10336494.